Osteoarthritis and Cartilage 27 (2019) 932–944

Osteoarthritis and Cartilage

Maintenance of SOX9 stability and ECM homeostasis by selenium-sensitive PRMT5 in cartilage

M. Sun † ‡, S. Hussain † ‡, Y. Hu † ‡, J. Yan † ‡, Z. Min † ‡, X. Lan † ‡, Y. Guo † ‡, Y. Zhao † ‡, H. Huang † ‡, M. Feng † ‡, Y. Han † ‡, F. Zhang † ‡, W. Zhu † ‡, L. Meng † ‡, D. Li † ‡, J. Sun † ‡ *, S. Lu † ‡ **

† *Department of Biochemistry and Molecular Biology, School of Basic Medical Sciences, Xi'an Jiaotong University Health Science Center, Xi'an, Shaanxi 710061, PR China*
‡ *Key Laboratory of Environment and Genes Related to Diseases (Xi'an Jiaotong University), Ministry of Education, Xi'an, Shaanxi, PR China*

ARTICLE INFO

Article history:
Received 16 October 2018
Accepted 27 February 2019

Keywords:
Selenium deficiency
PRMT5
SOX9
Extracellular matrix metabolism
Cartilage

SUMMARY

Objectives: Selenium (Se) plays pivotal roles in maintaining optimal health. Nevertheless, how Se influences the metabolism of extracellular matrix (ECM) in cartilage remains unclear. The aim of the present study was to observe protein dimethylation by certain Se-sensitive PRMT and to elucidate its effects on the key transcriptional factor in cartilage.
Methods: We observed the expression of selenoproteins and markers of ECM metabolism in chondrocytes and articular cartilage of the rats under Se-deficiency by RT-qPCR, immunoblotting and immunohistochemistry. Then, we analyzed the expression of total dimethylated protein by using specific antibody under different Se statuses. After Se sensitive PRMT was identified, we used siRNA or PRMT inhibitor or stably overexpressing vector to intervene in the PRMT expression and identified the key transcriptional factor. Co-immunoprecipitation was applied to verify the interaction between PRMT and the key transcriptional factor. Finally, we measured the half-life time of the key transcriptional factor by immunoblotting after cycloheximide treatment.
Results: In chondrocytes and cartilage of the rats with Se deficiency, we found an aberrant metabolism manifesting decreased expression of *Col2a1* and increased expression of *Mmp-3*. Then, we identified that PRMT5 was the unique type II PRMT, sensitive to Se status. PRMT5 upregulation led to the increased *COL2A1* expression but decreased *MMP-3* expression in chondrocytes. Furthermore, we revealed that PRMT5 improved SOX9 stability by dimethylating the protein, which contributed to maintain the matrix metabolic homeostasis of the chondrocytes.
Conclusions: Se-sensitive PRMT5 increases the half-life of SOX9 protein via PTM and helps to maintain ECM homeostasis of the articular cartilage.

Introduction

Selenium (Se), the essential trace element, plays an important role for humans[1]. Se is required for thyroid hormone metabolism, male reproduction, immune function, anti-inflammation, and the well-known functions in detoxifying free radicals[2–5]. Se-deficiency is associated with a compromised immune system and increased susceptibility to various diseases including arthritis, cancer, cardiovascular disease, cataracts, cholestasis, cystic fibrosis, diabetes, lymphoblastic anaemia, macular degeneration, muscular dystrophy, stroke and some others[1,6]. Se exerts its biological effects through selenoproteins (SeP). Selenocystein (Sec) – an activated form of Se, is incorporated into SeP by recoding UGA as a Sec codon rather than using as the conventional stop codon[7–10]. SeP synthesis requires a variety of components including the assembly of RNA–protein (RNP) complexes, Selenocysteine Insertion Sequences (SECIS), and SECIS binding protein 2 (SBP2)[11–13]. Low Se intake in

* Address correspondence and reprint requests to: J. Sun, Department of Biochemistry and Molecular Biology, School of Basic Medical Sciences, Xi'an Jiaotong University Health Science Center, Xi'an, Shaanxi 710061, PR China.
** Address correspondence and reprint requests to: S. Lu, Department of Biochemistry and Molecular Biology, School of Basic Medical Sciences, Xi'an Jiaotong University Health Science Center, Xi'an, Shaanxi 710061, PR China.
E-mail addresses: sunjian1@mail.xjtu.edu.cn (J. Sun), lushemin@mail.xjtu.edu.cn (S. Lu).

https://doi.org/10.1016/j.joca.2019.02.797
1063-4584/

Se-deficient areas has been proposed to have roles in the pathogenesis of Kashin-Beck disease (KBD), an endemic osteoarthropathy characterized by chondronecrosis in the deep zone of growth plate and articular cartilage. Deletion of Sec tRNA gene (Trsp) exhibits unbalanced cartilage matrix metabolism, chondronecrosis and abnormal skeletal development[14]. The pathological changes exhibited by Trsp depleted mice are similar to those observed in patients with KBD endemic in the Northern China[15,16]. Se levels in food and serum of individuals from KBD-affected areas are much lower than those in non-KBD areas[14,17]. Meanwhile, Se-supplementation has effectively prevented KBD occurrence[18–20].

Environmental factors like Se are believed to exert their biological influence through post-translational modification (PTM)[21]. Arginine can be dimethylated in a symmetrical (symmetrical dimethylated arginine, sDMA) or asymmetrical (asymmetrical dimethylated arginine, aDMA) manner. Protein arginine methyltransferase (PRMTs) type II including PRMT5, PRMT7 and PRMT9, form symmetric di-methyl-arginine. PRMT5 depleted mouse embryonic buds show severely truncated bones with wispy digits lacking joints[22], therefore its mechanisms in cartilage need further elucidating.

Articular cartilage is composed of chondrocytes and extracellular matrix (ECM). Of the regulatory factors controlling the phenotype of cartilage, transcriptional factors including SRY-box 9 (*Sox9*), Runt-related transcription factor 2 (*Runx-2*)[23], hypoxia and hypoxia inducible factor (*HIF-1*), and *Foxo3A* play crucial roles in maintenance of the homoeostasis of cartilage ECM, and the survival of chondrocytes[24–27]. Meanwhile, matrix-degrading enzymes such as matrix metalloproteinases (MMPs) and a disintegrin and metalloproteinase with thrombospondin motifs (ADAMTS) take responsibility to degrade the specific cartilage ECM components[28,29]. Overexpression of *MMPs* cleaves the ECM components of collagen II (COL2A1), X (COL10A1) and aggrecan (ACAN). Secretion of MMP-3 is an important characteristic of degrading cartilage along with bone matrix deterioration[30,31].

Previous study has showed that Se-deficiency leads to the epiphyseal plate lesion and SBP2 as a Se-sensitive marker regulates SeP expression in cartilage[32,33]. In this study, we aimed to elucidate the role and mechanism of PTMs in cartilage ECM homeostasis under Se-deficient conditions. GPx1 and SELS were selected as Se phenotype markers, as they are regulated by Se-deficiency and Se-sufficiency. In addition, we found that PRMT5 is the unique member of type II PRMTs, which is affected by Se status and may regulate cartilage ECM metabolism. Thus, the detailed regulatory relationship among “low-Se, PRMT5 and ECM metabolism in cartilage” was investigated.

Material and methods

Cell lines and culture condition

C28/I2, the human juvenile costal chondrocyte was obtained from Dr Mary B. Goldring, kept in DMEM/F-12 (HyClone, catalog SH30261.01) containing 10% fetal bovine serum (FBS; ExCell, FCS500) and passaged three times a week. SW1353 cell line was obtained from American Tissue Culture Collection (ATCC, USA), kept in RPMI-1640 medium (HyClone, catalog SH30809.01) containing 10% FBS and passaged two or three times a week. All cell lines were detached by treatment with 0.25% trypsin (ExCell, CB000-C022). The medium with 1% penicillin/streptomycin (Thermo Fisher, catalog 15140122) was changed every 2 days.

All cell lines used for Se-sufficient (Se-S) and Se-deficient (Se-D) cultures, were first pre-cultured in medium supplemented with 1% FBS (5 nM of Se in the culture medium estimated by atomic absorption spectroscopy) at least for 5 days resulting in Se-D condition, and subsequently replaced by medium containing sodium selenite (Sigma, catalog S5261-10G, 50 nM) for over 24 h in Se-S condition according to our previous protocol[34,35].

Rats

DA rats were bred and kept in the animal house of Department of Biochemistry and Molecular Biology, Xi'an Jiaotong University Health Science Center. The two generation Se-deficient rat model was established as described previously[32]. The experiments were approved by Institutional Animal Ethics Committee of the University (Permission ID: XJ2006Y039; Xi'an Jiaotong University, Xi'an, China) and were in compliance with ARRIVE guidelines and European Community specifications regarding the use of laboratory animals.

Small interfering RNA

Human *PRMT5* and *SBP2* siRNA sequences and the scrambled (NC) siRNA sequence were obtained from Genepharma Co., Ltd (Shanghai, China). C28/12 cells were plated in 12-well plates, kept in DMEM/F-12 medium without FBS and antibiotics. Next day, cells were transfected with *PRMT5* siRNA or *SBP2* siRNA and scrambled siRNA using Lipofectamime 2000 transfection reagent (Thermo Fisher, catalog 11668-019, 2μl/well) in accordance with the manufacturer's instructions. Protein and mRNA samples were collected for further detection after transfection. The siRNA sequences used in this study were: *SBP2* sense: 5′-GAGCCACACUACAUUGAAATT-3′, *SBP2* antisense: 5′-UUUCAAUGUAGUGUGGCUCTT-3’; *PRMT5* sense: 5′-CCAGUUUGAGAUGCCUUAUTT-3′, *PRMT5* antisense: 5′-AUAAGGCAUCUCAAACUGGTT-3′.

Adeno-virus vector infection

Human *SBP2* or *PRMT5* cDNA was cloned and inserted into pHBAd-MCMV-GFP expression vector with GFP from Hanbio Biotechnology Co., Ltd (Shanghai, China). Empty vectors were used as the controls. C28/12 cells were plated in 12-well plates cultured in DMEM/F-12 medium without FBS and antibiotics. Reaching the 70% confluency, the cells were infected with pHBAd-MCMV-GFP-SBP2 (*ad-SBP2*) or pHBAd-MCMV-GFP-PRMT5 (*ad-PRMT5)* and control (*ad-NC)* according to the manufacturer's instructions. The recombinant adenoviruses were directly added into the culture medium (300 MOI/well) and incubated for 4–6 h, followed by replacing the medium by complete medium with no adenovirus vector. Protein and mRNA samples were collected for further analysis after the virus vector infection.

DNA plasmid transfection

Human $SOX9^{WT}$ CDS, $SOX9^{R74K}$ CDS, $SOX9^{R177K}$ CDS and $SOX9^{R177K}$ CDS were cloned from chondrocyte cDNA of SW1353 cell lines and inserted into pcDNA3.1 vector (Thermo Fisher, catalog VPI0001) with FLAG tag in the N-terminal. Primer sequences used for $SOX9^{WT}$ CDS, $SOX9^{R74K}$ CDS, $SOX9^{R177K}$ CDS and $SOX9^{R177K}$ CDS clones are listed in Table S1.

SW1353 cells were seeded in 12-well plates, at 70% confluence, pcDNA3.1-FLAG-SOX9 ($SOX9^{WT}$) (2μg/well) or pcDNA3.1-FLAG-$SOX9^{R74K}$ ($SOX9^{R74K}$) (2μg/well) or pcDNA3.1-FLAG-$SOX9^{R177K}$ ($SOX9^{R177K}$) or pcDNA3.1-FLAG-$SOX9^{R179K}$ ($SOX9^{R179K}$) (2μg/well) vectors were transiently transfected into cells by Lipofectamine 2000.

Real-time quantitative PCR

RT-qPCR assay was performed for detection of relative gene expression. Total mRNA from cells or cartilage tissues of DA rats were isolated using TRIzol reagent (Thermo Fisher, catalog 15596-026) according to the manufacturer's instructions. Subsequently, reverse transcription was performed using the Transcriptor cDNA Synthesize Kit (Roche, catalog 04897030001). Gene expression was performed on Agilent real-time PCR detection system (Agilent tech. USA) with SYBR Premix-Fast Start Universal SYBR Green Master (Rox) (Roche, catalog 04913850001). Quantification of the relative expression levels was determined by $\Delta\Delta^{Ct}$ method. The relative gene expression was normalized by *GAPDH*. The information of primers is depicted in Table S2.

Inhibition of PRMT5 activity

C28/12 cells were plated in 12-well plates, and treated with PRMT5 inhibitor (EPZ015666, Selleck, catalog S7748, 5 nM) for 48 h. Protein and mRNA samples were collected for further detection after PRMT5 inhibitor treatment.

Immunoblotting

C28/12 cells were harvested by immunoblotting lysis buffer (Beyotime, catalog P0012B) containing protease inhibitor mixture (Bimake, catalog B14002). The lysates were incubated on ice for 30 min followed by centrifugation at 12,000 *g* for 12 min to remove cellular debris. The supernatants were transferred into clean 1.5 ml tubes. The protein concentration in the supernatant was determined by bicinchoninic acid (BCA) method (TIANGEN, catalog PA115). Cellular extracts were mixed with SDS loading dye (Thermo Fisher, catalog R1151), heated at 95°C for 5min, 15 μg of the protein sample loaded into SDS-polyacrylamide gels, and subjected to gel electrophoresis (SDS-PAGE). Subsequently proteins were electro-transferred to polyvinylidene difluoride (PVDF) membranes (Millipore, catalog IPVH00010). The membrane was blocked with 5% (w/v) milk for 2 h and incubated with primary antibody at 4°C overnight. The antibody information is depicted in Table S3. After primary antibodies incubation, the membrane was washed 3 times with TBST (TBS+0.1% Tween) and incubated with horseradish peroxidase-conjugated anti-mouse (1:10,000, catalog A21202), or anti-rabbit (1:10,000, catalog A11036) secondary antibodies (from Thermo Fisher) for an hour. Excessive secondary antibody conjugated with HRP was then rinsed off by washing the membrane 3 times with TBST. The membrane was visualized by ECL reagents (Millipore, catalog MA01821). Immunoblotting were scanned by GeneGnome XRQ System with the GeneTools analysis software (Syngene, MD, USA), and densitometry of specific immunoblotting bands was analyzed with the GeneTools analysis software.

Co-immunoprecipitation

C28/I2 cells were harvested by immunoprecipitation lysis buffer (Beyotime, catalog P0012B) containing protease inhibitor mixture (Bimake, catalog B14002). The lysates were incubated on ice for 30 min and centrifuged at 12,000×*g* for 12min to remove cellular debris. The supernatants were transferred into clean 1.5 ml tubes. The antibodies were added to protein extracts in 1.5 ml EP tubes and incubated at 4°C overnight with gentle rotation. IgA- or IgG-agarose beads (Beoytime, catalog P2012) were added to the extracts and incubated at 4°C for 3 h with gentle rotation for antibody-bead coupling. The beads were washed with PBS for 3 times to remove unbound proteins. SDS loading dye (Thermo Fisher, catalog R1151) was added to the protein complexes. Protein complexes were then heated at 95°C for 5min. Eluted proteins were detected by immunoblotting. The antibody information is depicted in Table S3.

Immunohistochemistry staining

DA rats cartilage tissues were fixed in 4% buffered paraformaldehyde for more than 2 days and subsequently decalcified with EDTA (12.5% EDTA, pH 7.4). Cartilage tissue sections were embedded in paraffin and 4 μm-thick sections were cut. Immunohistochemistry staining was performed using the standard streptavidin peroxidase complex method. Firstly, tissue sections were deparaffinized in xylene and rehydrated through a graded series of alcohols. Next, tissue sections were subjected to H_2O_2 treatment and antigen retrieval, and subsequently blocked with 5% bovine serum albumin (BSA) for 30 min at room temperature. Tissue sections were incubated with primary antibodies at 4°C overnight. After sequential incubations with biotinylated secondary antibody (BOSTER, catalog SA1022, China) and horseradish peroxidase-conjugated avidin (BOSTER, catalog SA1022, China), protein staining was performed using the Diaminobenzidine Substrate Kit (BOSTER, catalog SA2022, China). Samples were counterstained with hematoxylin, and the resulting brown staining indicated the proteins immunoreactivity. The results of IHC were observed under microscope with 400× magnification and quantification was performed with the Image-Pro® Plus software. The antibody information is depicted in Table S3.

Protein half-life time

C28/I2 or SW1353 cells were seeded in 12-well plates, resulting in 90% confluence. Cells were treated with PRMT5 inhibitor, EPZ015666 (5 nM, Selleck, catalog, S774) or DMSO for 48 h. The cells were infected with *ad-PPRMT5* or *ad-NC* for 48 h. Next, cells were treated with cycloheximide (CHX; Sigma, catalog 66-81-9, 50 μg/ml) or DMSO and subsequently harvested at 0, 1, 2, 3, 4 and 5 h post-treatment of cycloheximide for immunoblotting. The density from 0 h sample was measured by the software Image J and arbitrarily fixed as one to which those from other time points were compared and protein half-life time was calculated by $t_{1/2} = 0.693/k$ and $k = (Inc_o\text{-}Inc)/t$.

Statistics

Data were expressed as mean ± 95% confidence intervals. Statistical analysis of multiple groups was undertaken using one-way ANOVA with Tukey adjusted pairwise comparisons. Differences between two groups were performed by Student's *t* test. The Mann-Whitney *U* test was used to analyze the density of immunoblotting bands and the positive cells of immunohistochemistry staining. Correlation analysis was carried out by Spearman test. $P < 0.05$ was considered as statistically significant.

The effect animal number was calculated for unequal sample size based on the mean difference between Se-S and Se-D groups by OpenEpi303 online software. A sample of 12 rats was considered appropriate balancing resources with a desire to limit animal expenditure. Although the analysis was considered exploratory, such a sample is sufficient to determine statistically significant differences of 1.8–5.6 standard deviations between Se-S and Se-D groups using 2–6 experimental units per group with 80% power and at a significance level of 0.05. Differences of this magnitude would be considered large, but are not uncommon in these types of experiment.

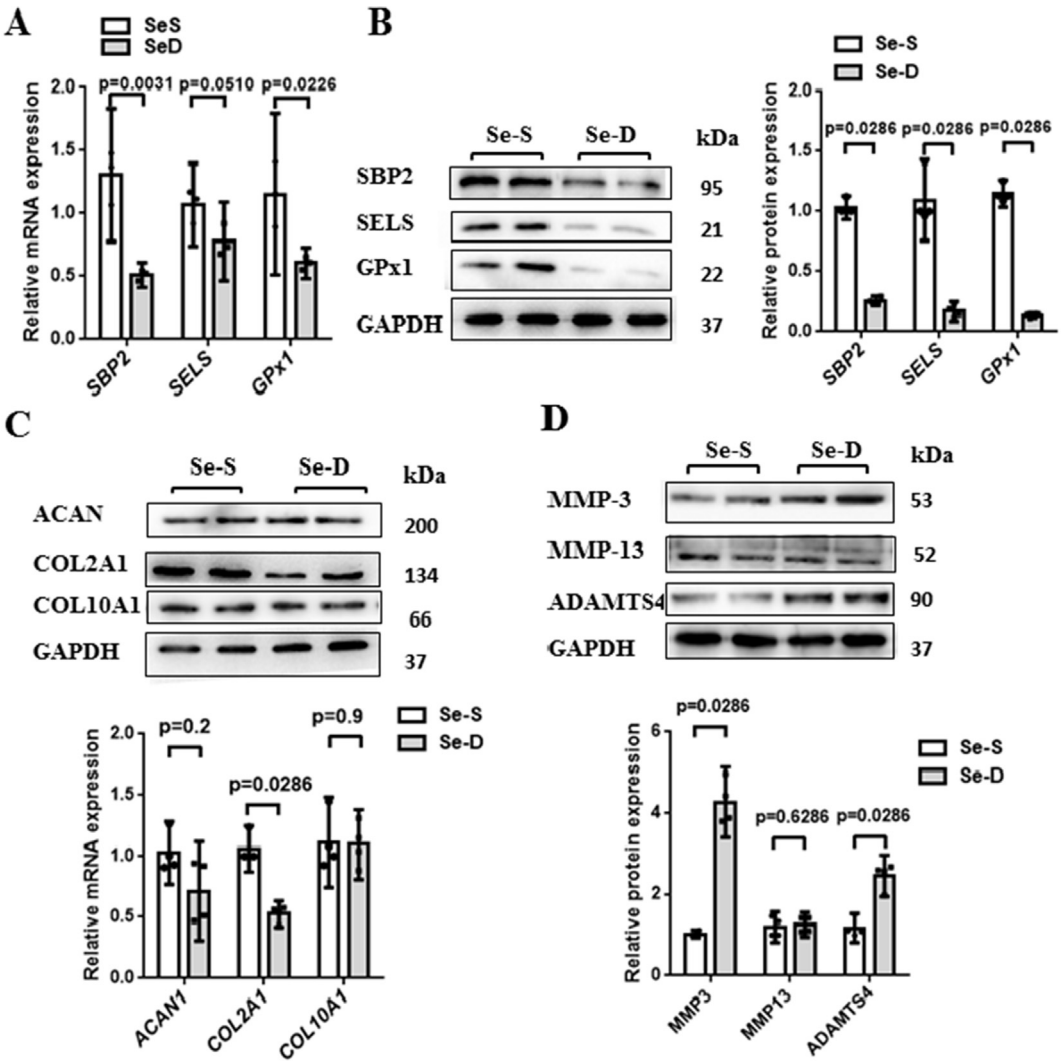

Fig. 1. Se-deficiency leads to abnormal ECM metabolism. **A.** C28/I2 cells were cultured in Se sufficient (Se-S) and Se deficient (Se-D) media, and mRNA levels of *SBP2*, *SELS* and *GPx1* were detected by RT-qPCR. ($n = 3$) **B.** C28/I2 cells were cultured in Se-S and Se-D media. The lysates were immunoblotted with the antibodies against SBP2, SELS and GPx1. ($n = 4$) **C.** C28/I2 cells were incubated with Se-S and Se-D media. The lysates were immunoblotted with the antibodies against ACAN, COL2A1, and COL10A1. ($n = 4$) **D.** C28/I2 cells were treated with Se-S and Se-D media. The lysates were immunoblotted with the antibodies against MMP-3, MMP-13, and ADAMTS-4. ($n = 4$) Glyceraldehyde-3-phosphate dehydrogenase (GAPDH) was used as an internal control in RT-qPCR and immunoblotting detections. Immunoblotting (IB) bands were analyzed quantitatively by Image J. software. All the values were obtained from the mean of three separate repeated experiment results for statistic. Data are presented as mean ± 95 % Cl and analyzed using Student's *t*-test (A) and Mann-Whitney *U* test (B-D).

Results

Se-deficiency leads to abnormal ECM metabolism

Se, the trace element nutrient is required during cartilage development. We asked whether Se-deficiency plays a role in the ECM metabolism, we developed a Se-deficiency cell model in depleted intracellular Se (serum deprivation preconditioning for 5 days) but not those under standard culture conditions because serum already contains sufficiency trace amounts (about 500 nM) of Se. Our previous study showed that SBP2 is a Se-sensitive gene, which can evaluate the Se statues in chondrocytes. Therefore, we detected SBP2, *GPx1* and SEL S to confirm the Se statues in chondrocytes, results from human C28/I2 chondrocyte line showed that mRNA expression of *SBP2* and *GPx1* was significantly down-regulated in Se-D group as compared to Se-S group, while *SEL S* expression seemed not to be changed significantly [Fig. 1(A)]. But at protein level, the expression of *SEL S* was inhibited significantly along with *SBP2*, *GPx1* in Se-D group as compared to Se-S group [Fig. 1(B)]. We also used rat C5.18 chondrocyte line and obtained the same results [Fig. S1(A)]. Next, we examined protein levels of *ACAN, COL2A1* and *COL10A1* (the molecular markers of chondrocyte anabolic phenotype), and MMP-3, MMP-13 and ADAMTS-4 (the molecular markers for chondrocyte catabolic phenotype). Results showed that *COL2A1* expression decreased [Fig. 1(C)] as well as *MMP-3* and *ADAMTS-4* expression increased significantly in Se-D group as compared to Se-S group [Fig. 1(D)]. In addition, *MMP-13* and *COL10A1* expression did not change between two groups. The same results were obtained from rat C5.18 chondrocyte line [Figs. S1(B) and (C)]. These results indicate that Se-deficiency accelerates chondrocyte ECM degradation.

Se-sensitive SBP2 affects symmetric di-methylation of proteins in chondrocytes

To confirm whether Se affects the proteins that contain sDMA at steady state, an sDMA-specific antibody SYM10 was used. SYM10

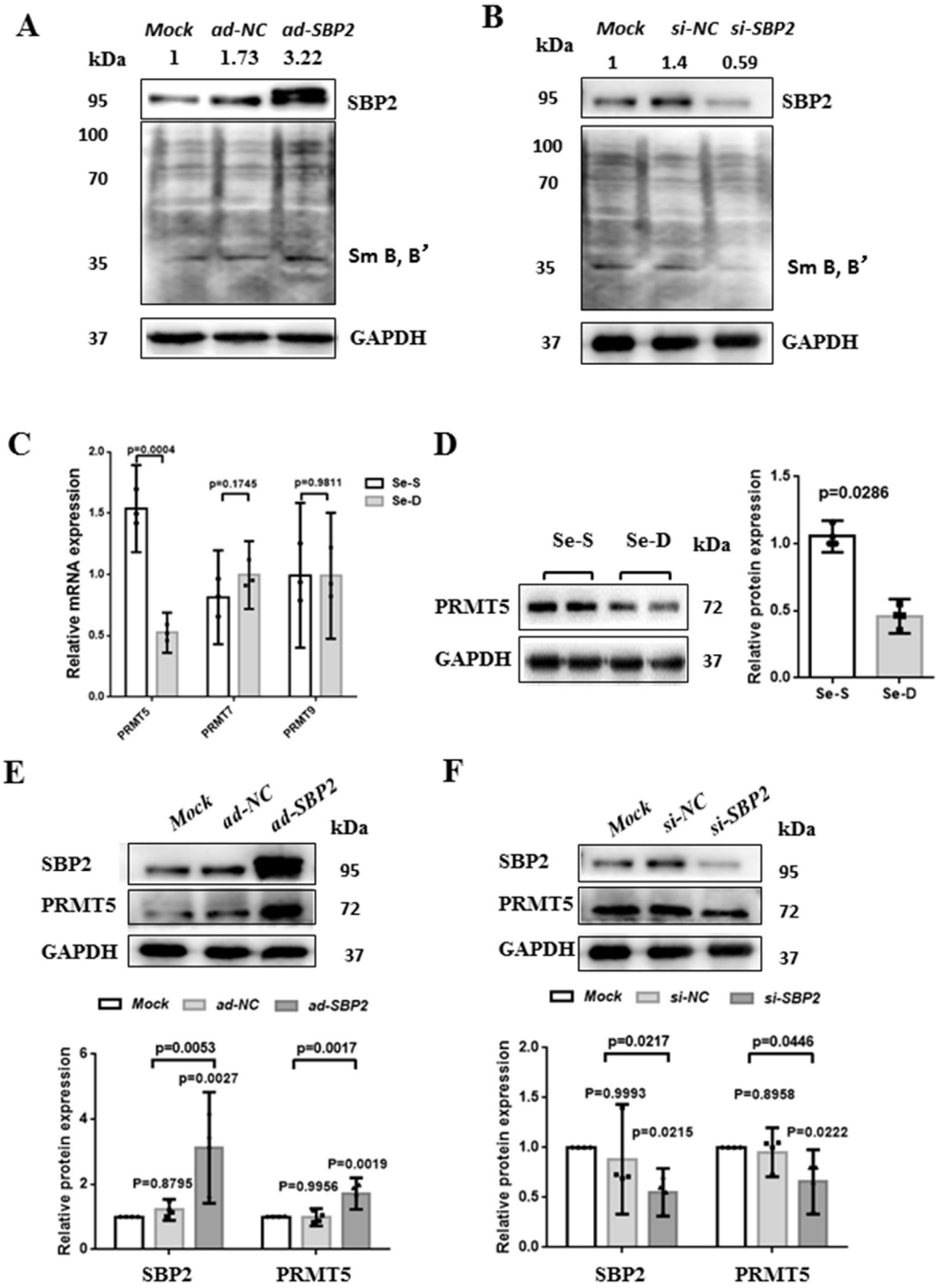

Fig. 2. PRMT5 is down-regulated in chondrocyte with Se deficiency *in vitro*. **A.** C28/I2 cells were treated with control adeno-virus (*ad-NC*), or *SBP2* overexpressing adeno-virus (*ad-SBP2*) or no adeno-virus (*Mock*). SBP2 and dimethylated protein expression in chondrocytes was detected by immunoblotting with the antibodies against SBP2 and symmetric dimethyl arginine (SYM10). ($n = 3$) **B.** C28/I2 cells were treated with scrambled siRNA (*si-NC*) or SBP2 siRNA (*si-SBP2*) or no siRNA (*Mock*). ($n = 3$) Protein levels of SBP2 and SYM10 were detected by immunoblotting with SBP2 and SYM10 antibodies. **C.** C28/I2 cells were treated with Se-S and Se-D media, and mRNA levels of *PRMT5*, *PRMT7* and *PRMT9* were detected by RT-qPCR. ($n = 3$) **D.** C28/I2 cells were cultured in Se-S and Se-D media. The lysates were immunoblotted with the antibody against PRMT5. ($n = 4$) E. C28/I2 cells were treated with control adeno-virus (ad-NC), or SBP2 overexpressing adeno-virus (ad-SBP2) or no adeno-virus (Mock). SBP2 and PRMT5 expression in chondrocytes was detected by immunoblotting with the antibodies against SBP2 and PRMT5. ($n = 4$) F. C28/I2 cells were treated with scrambled siRNA (*si-NC*) or SBP2 siRNA (*si-SBP2*) or no siRNA (*Mock*). ($n = 4$) Protein levels of SBP2 and PRMT5 were detected by immunoblotting with SBP2 and PRMT5 antibodies. GAPDH was used as an internal control in RT-qPCR and immunoblotting detections. Intensities of IB protein bands were calculated by Image J software and normalized with GAPDH. All the values were obtained from the mean of three separate repeated experiment results for statistic. Data are presented as mean ± 95 % CI and analyzed using Student's *t*-test (C), Mann-Whitney *U* test (D) and one-way ANOVA followed by Tukey test (E and F).

recognized methylated SmB', B proteins[36], as in Fig. 2(A) and (B) also showed the same results. We intervened *SBP2* expression to change Se status and subsequently used SYM10 to detect proteins containing sDMA. Results showed that overexpression of *SBP2* increased the expression of proteins containing sDMA, significantly observed at 70–100 kDa [Fig. 2(A)]. On the other hand, *SBP2*

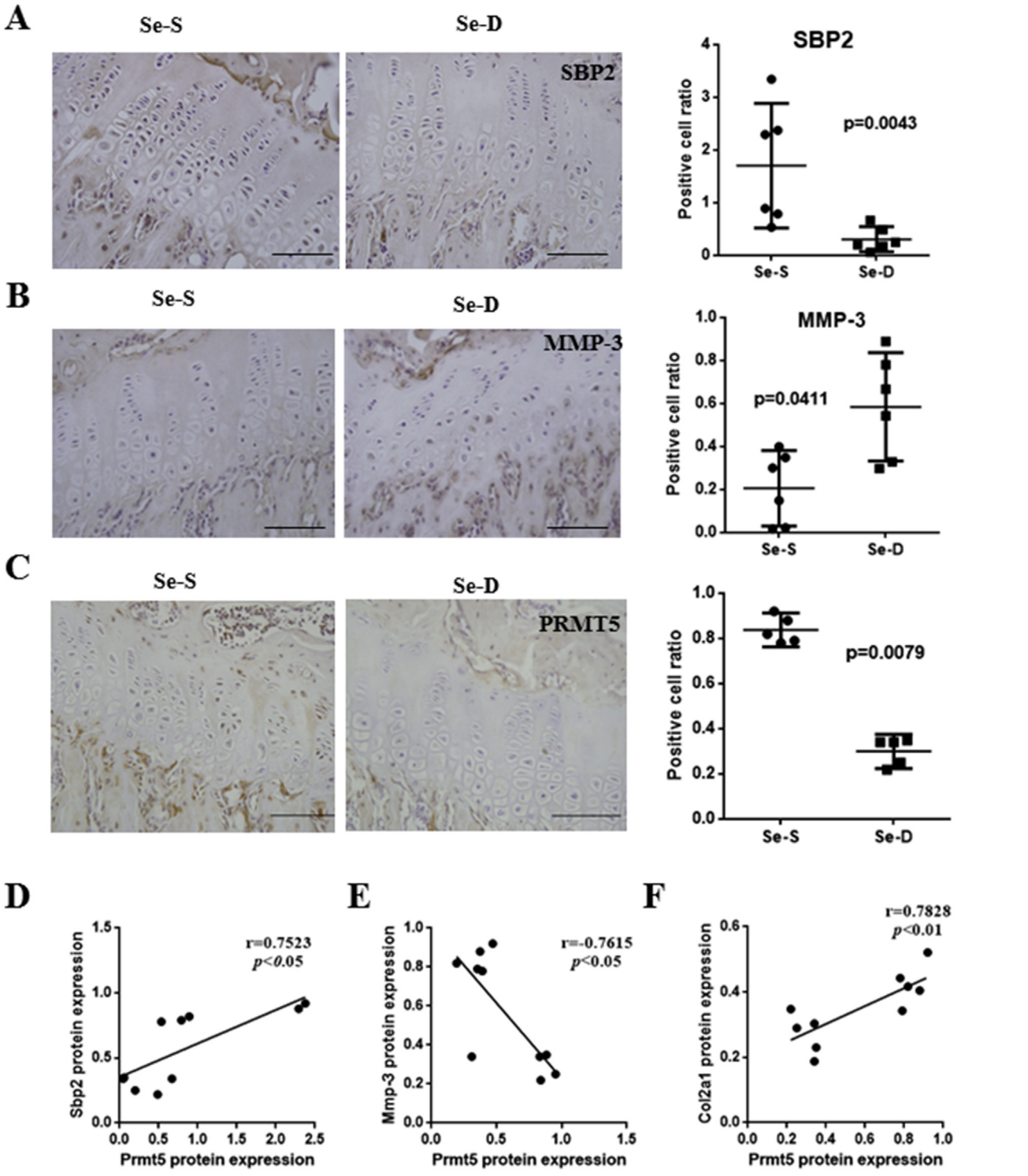

Fig. 3. PRMT5 is down-regulated in chondrocyte with Se deficiency *in vivo*. **A.** Representative pictures of immunohistochemical staining, showing protein expression of *Sbp2* using SBP2 antibody, in cartilage tissues from two generation DA rats fed with Se-S ($n = 6$) and Se-D ($n = 6$) diets (left panel). Scale bar, 100 μm. The relative protein expression of *Sbp2* in Se-D and Se-D groups was calculated from the percentages of SBP2 positive chondrocytes (right panel). **B.** Representative pictures of immunohistochemical staining, showing protein expression of *Mmp-3* using MMP-3 antibody in cartilage tissues from two generation DA rats fed with Se-S ($n = 6$) and Se-D ($n = 6$) diets (left panel). Scale bar, 100 μm. The relative protein expression of *Mmp-3* was calculated from the percentages of MMP-3 positive chondrocytes (right panel). **C.** Representative pictures of immunohistochemical staining, showing protein expression of *Prmt5* in cartilage tissues from two generation DA rats fed with Se-S ($n = 5$) and Se-D ($n = 5$) diets (left panel). Scale bar, 100 μm. The relative protein expression *Prmt5* was calculated from the percentages of PRMT5 positive chondrocytes (right panel). **D.** Correlation analysis between the percentages of SBP2-positive and PRMT5-positive chondrocytes in the samples from Se-S and Se-D groups ($n = 10$) was performed by Pearson's correlation ($r = 0.7523$, $P < 0.05$). **E.** Correlation analysis for the percentages between MMP-3-positive and PRMT5-positive chondrocytes in samples from the Se-S and Se-D groups ($n = 10$), performed by using Pearson's correlation ($r = 0.7615$, $P < 0.05$). **F.** Correlation analysis for the percentages of COL2A1-positive and PRMT5-positive chondrocytes in samples from the Se-S and Se-D groups ($n = 10$), performed by Pearson's correlation ($r = 0.7828$, $P < 0.01$). All the values were obtained from the mean of three separate repeated experiment results for statistic. Data are presented as mean ± 95 % Cl and analyzed using Mann-Whitney *U* test (A-C) and correlation analysis was carried out by Spearman test (D-F).

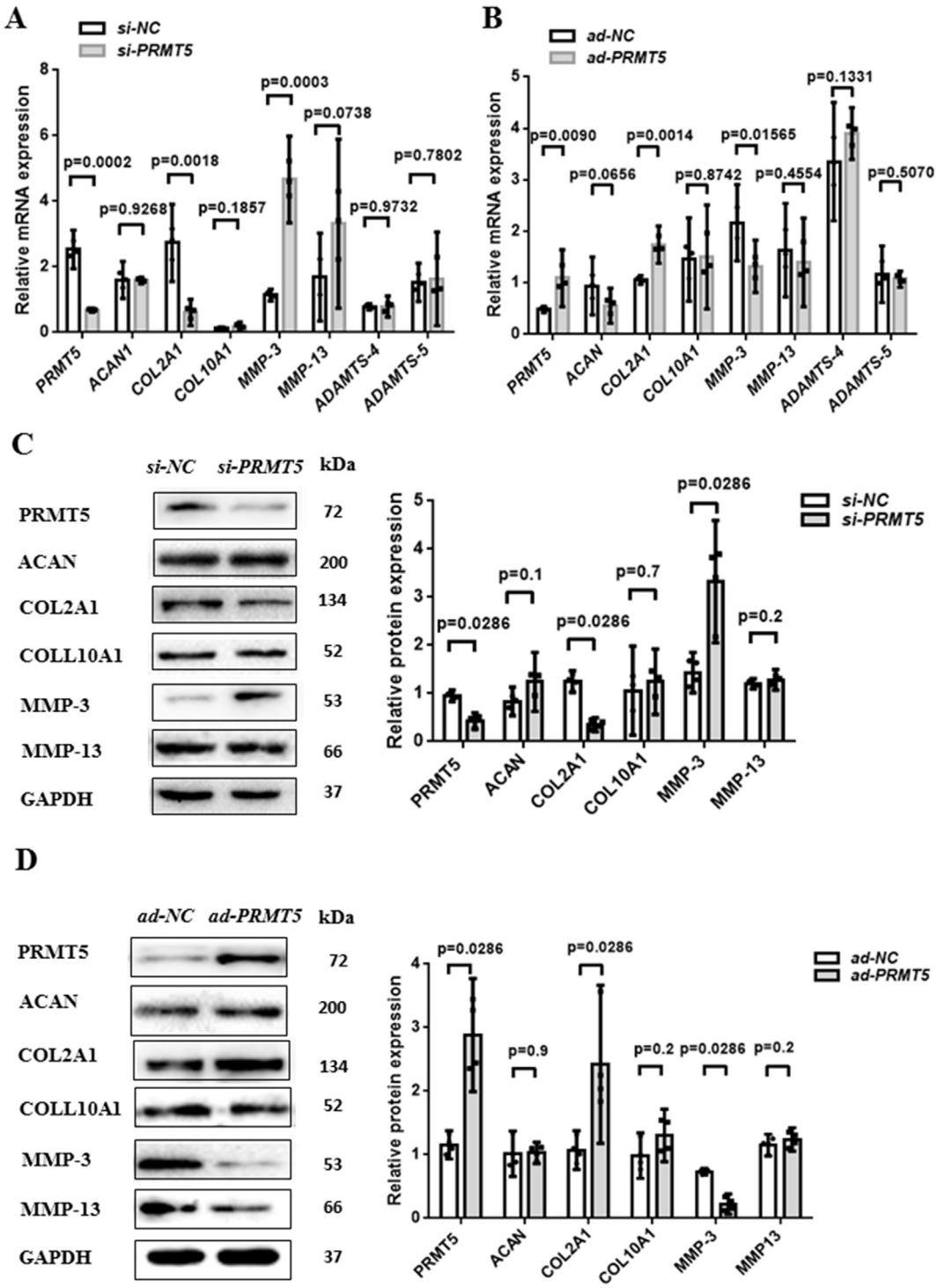

Fig. 4. PRMT5 maintains ECM homeostasis in chondrocytes. **A.** C28/I2 cells were treated with scrambled siRNA *(si-NC)* or PRMT5 siRNA (*si-PRMT5*). *PRMT5*, *ACAN*, *COL2A1, COL10A*, *MMP-3*, *MMP-13*, *ADAMTS-4* and *ADAMTS-5* mRNA expressions were detected by RT-qPCR. ($n = 3$) **B.** C28/I2 cells were treated with control adeno-virus (*ad-NC*) or *PRMT5* over-expressing adeno-virus vector (*ad-PRMT5*). *PRMT5*, *ACAN*, *COL2A1*, *COL10A1*, *MMP-3*, *MMP-13*, *ADAMTS-4* and *ADAMTS-5* expressions were detected by RT-qPCR. ($n = 3$) **C.** 28/I2 cells were treated with scrambled siRNA *(si-NC)* or PRMT5 siRNA (*si-PRMT5*). Protein expression of *PRMT5*, *ACNA, COL2A1, COL10A1, MMP-3 and MMP-13* was determined by immunoblotting with respective antibodies. ($n = 4$) **D.** C28/I2 cells were treated with control adeno-virus (*ad-NC*) or *PRMT5* overexpression adeno-virus (*ad-PRMT5*). Protein expression of *PRMT5*, *ACNA, COL2A1, COL10A1, MMP-3 and MMP-13* was determined by immunoblotting with respective antibodies. ($n = 4$) GAPDH was used as an internal control in RT-qPCR and immunoblotting detections. Intensities of IB protein bands were calculated by Image J software and normalized with GAPDH. All the values were obtained from the mean of three separate repeated experiment results for statistic. Data are presented as mean ± 95 % CI and analyzed using Student's *t*-test (A and B) and Mann-Whitney *U* test (C and D).

knockdown inhibited the expression of proteins containing sDMA, observed at 70–100 kDa [Fig. 2(B)]. These results indicate that SBP2 affects the expression of proteins that contain sDMA in chondrocytes.

PRMT5 is down-regulated in chondrocytes with Se-deficiency

We found type II *PRMTs* are sensitive to Se-deficiency and may play roles in chondrocyte ECM metabolism, we thus screened the

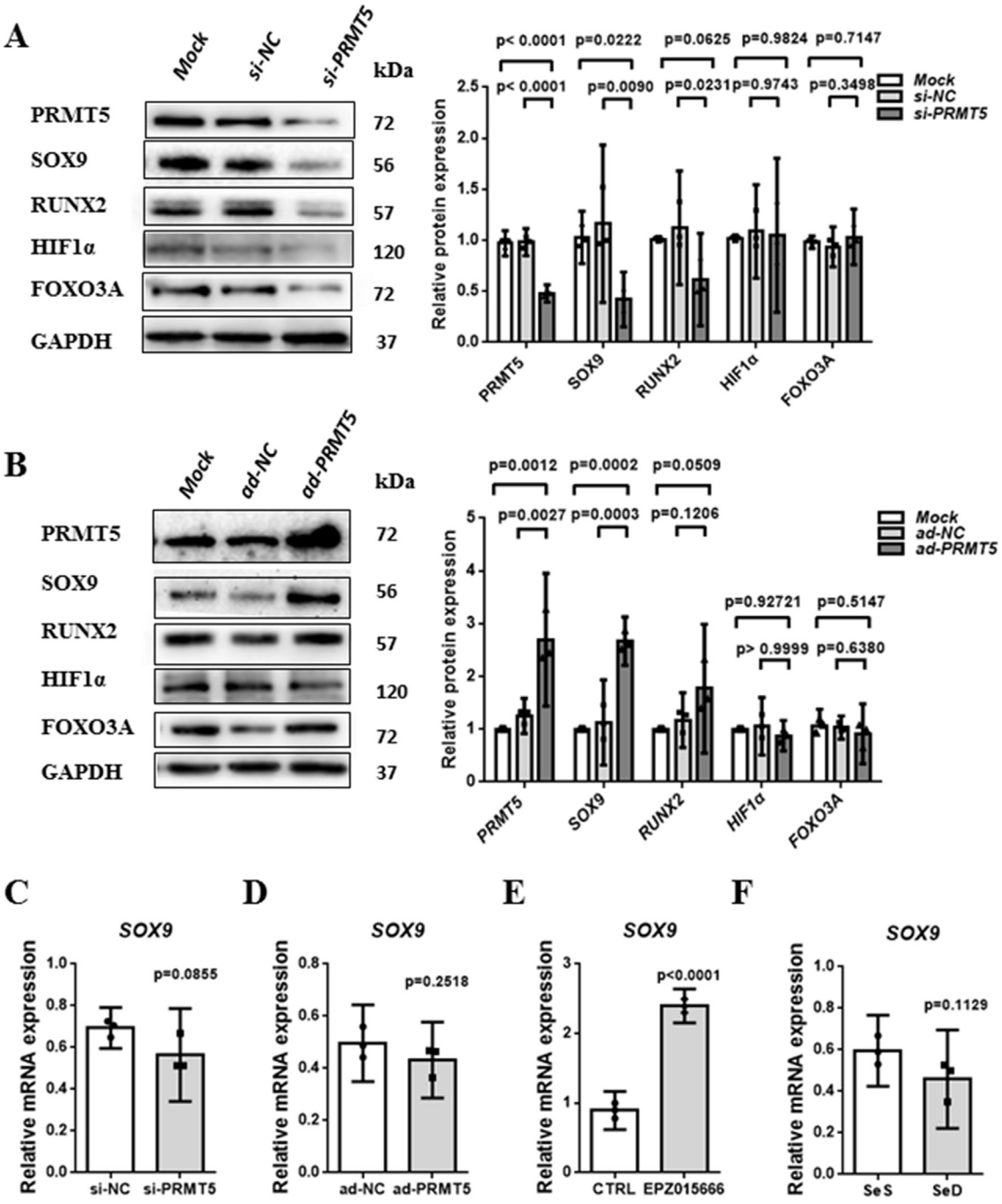

Fig. 5. PRMT5 positively regulates SOX9 to maintain ECM homeostasis in chondrocytes. **A.** C28/I2 cells were treated with scrambled siRNA *(si-NC)* or PRMT5 siRNA (*si-PRMT5*) or no siRNA (*Mock*). Protein expressions of *PRMT5*, *SOX9*, *RUNX2*, *HIF1a*, and *FOXO3A* were determined by immunoblotting with respective antibodies. ($n = 3$) **B.** C28/I2 cells were treated with control adeno-virus (*ad-NC*) or *PRMT5* overexpressing adeno-virus vector (*ad-PRMT5*) or no vector treatment (*Mock*). Protein expressions of *PRMT5*, *SOX9*, *RUNX2*, *HIF1a*, and *FOXO3A* were determined by immunoblotting with respective antibodies. ($n = 3$) **C.** C28/I2 cells were treated with scrambled siRNA *(si-NC)* or PRMT5 siRNA (*si-PRMT5*), mRNA levels of *SOX9* were detected by RT-qPCR. ($n = 3$) **D.** C28/I2 cells were treated with non-targeting adeno-virus (*ad-NC*) or PRMT5 overexpressing adeno-virus (*ad-PRMT5*), mRNA levels of *SOX9* were detected by RT-qPCR. ($n = 3$) **E.** C28/I2 cells were treated with EPZ015666 or control, cultured in complete medium, mRNA levels of *SOX9* were detected by RT-qPCR. ($n = 3$) **F.** C28/I2 cells were cultured in Se-D and Se-S media, mRNA levels of *SOX9* were detected by RT-qPCR. ($n = 3$) GAPDH was used as an internal control in RT-qPCR and IB detections. Intensities of IB bands were quantitatively analyzed by Image J. software. All the values were obtained from the mean of three separate repeated experiment results for statistic. Data are presented as mean ± 95 % CI and analyzed using Student's *t*-test (C-F) and one-way ANOVA followed by Tukey test (A and B).

expression of typeII *PRMTs* in Se-deficiency condition, and observed that only *PRMT5* expression was decreased significantly in Se-D group as compared with Se-S group [Fig. 2(C) and (D)] in human chondrocytes (C28/I2). The same results were obtained from rat chondrocyte line C5.18 [Fig. S1(D)]. We further tested the expression of *PRMT5* after intervening *SBP2* expression. And results showed that SBP2 positively regulates *PRMT5* expression [Fig. 2(E) and (F)].

To further confirm whether PRMT5 is positively regulated by Se-deficiency *in vivo*, we developed Se-deficiency rat model and observed that the epiphyseal plate thicknesses of femurs and tibias from Se-D rats were significantly lessened than those from Se-S rats [Fig. S1(E)]. In two generation DA rats fed with Se-D diet, we observed that SBP2 was significantly inhibited as compared to Se-S group rats [Fig. 3(A)]. Contrarily, MMP-3 protein expression was

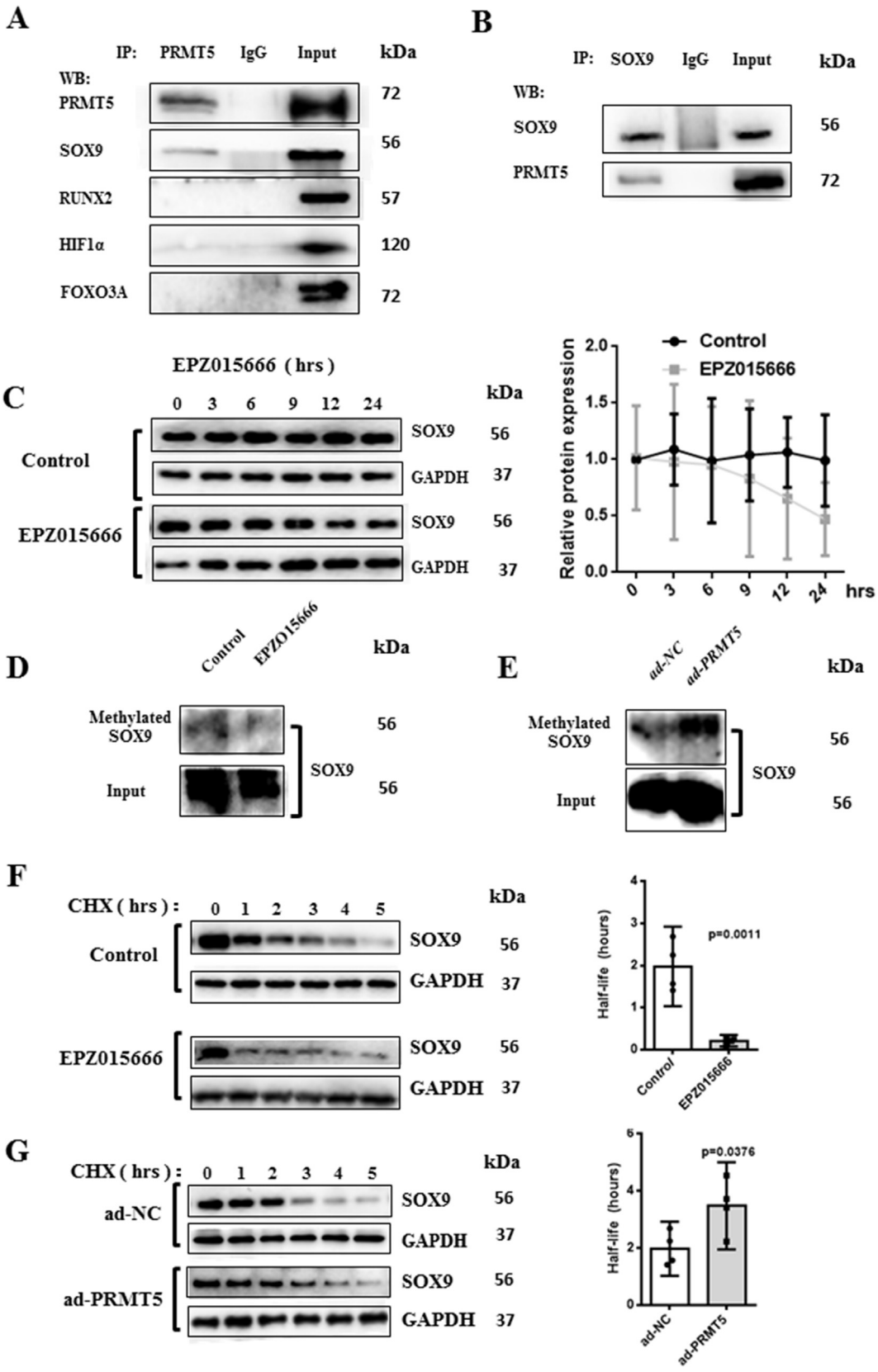

Fig. 6. PRMT5 methylates SOX9 to maintain its stability. **A.** C28/I2 cell lysates were immunoprecipitated with control IgG or PRMT5 antibodies, and subsequently immunoblotted with the indicated antibodies. ($n = 3$) **B.** Lysates from the cells were immunoprecipitated with control IgG or SOX9 antibodies, and subsequently immunoblotted with the indicated antibodies. ($n = 3$) **C.** C28/I2 cells were treated with EPZ015666 or control, cultured in complete medium. SOX9 protein levels were determined by immunoblotting using SOX9 antibody (left panel). Relative quantitation of SOX9 protein levels in chondrocytes from the control group compared with PRMT5 inhibitor group (right panel). ($n = 3$) **D.** C28/I2 cells were treated with PRMT5 inhibitor or control, cultured in complete medium. Cell lysates were immunoprecipitated with SYM10 antibody and subsequently immunoblotted with

significantly increased in Se-D cartilage tissues compared with Se-S cartilage tissues [Fig. 3(B)]. We have previously demonstrated a significant reduction of *Col2a1* expression in cartilage tissues from Se-D rats as compared with Se-S rats, and a significant increase of *Adamts-4* expression in cartilage tissues from Se-D rats compared with Se-S rats[32]. All the data evidently establish that Se-deficiency results in increased cartilage ECM degradation. Next, we checked the gene expression of *PRMT5* by RT-qPCR, and witnessed a significant down-regulation of PRMT5 in Se-D group rats [Fig. S1(F)]. From immunohistological sections, we observed that *PRMT5* expression was significantly inhibited in the epiphyseal plates of Se-D rats as compared to Se-S rats [Fig. 3(C)].

We performed the correlation analysis of *Prmt5* and *Sbp2* expression in the cartilage specimens from Se-S and Se-D rat groups. Results showed a positive relationship between *PRMT5* and *SBP2* in rat experiments [Fig. 3(D)]. Correlation analysis of *Prmt5* with *Mmp-3* as well as *Col2a1* was also determined. And we observed a significant negative correlation between *Prmt5* and *Mmp-3* while a significant positive correlation between *Prmt5* and *Col2a1* [Fig. 3(E) and (F)]. These results indicate that Se-deficiency inhibits *PRMT5* expression and increases the degradation enzyme expression in cartilage. Furthermore, PRMT5 is involved in regulating the homeostasis of ECM in cartilage.

PRMT5 maintains ECM homeostasis in chondrocytes

We knocked down or overexpressed *PRMT5* and detected the expression of key anabolic and catabolic markers, such as *ACAN*, *COL2A1*, *COL10A1*, *MMP-3*, *MMP-13*, *ADAMTS-4* and *ADAMTS-5* at mRNA level. Results showed that the expression of *MMP-3* was significantly increased after *PRMT5* knockdown [Fig. 4(A)], while *COL2A1* expression was significantly increased after *PRMT5* overexpression [Fig. 4(B)]. Data obtained at the protein level was consistent with the mRNA data, showing downregulation of COL2A1 while upregulation of MMP-3 expression after PRMT5 knockdown [Fig. 4(C)]. On the other hand, overexpression of *PRMT5* resulted in the upregulation of COL2A1 while downregulation of MMP-3 expression, as determined by immunoblotting [Fig. 4(D)]. These results indicate that PRMT5 increases *COL2A1* expression, but decreases *MMP-3* expression in chondrocytes.

PRMT5 positively regulates SOX9 to maintain ECM homeostasis in chondrocytes

Next, we detected important transcriptional factors expression in chondrocyte including SOX9, RUNX2, HIF1α and FOXO3A at protein level. We observed that after interfering *PRMT5* by siRNA, expression of *SOX9*, *RUNX2*, *HIF1*α and *FOXO3A* seemed to be down-regulated, SOX9 in particular, which was significantly decreased [Fig. 5(A)]. After overexpressing *PRMT5*, only *SOX9* expression was significantly enhanced [Fig. 5(B)]. We further observed SOX9 expression at mRNA level in different scenarios. After knockdown and overexpression of *PRMT5*, *SOX9* expression did not change at mRNA level [Fig. 5(C) and (D)]. Then we detected *SOX9* expression at mRNA level in Se-S and Se-D cells, and there was no change either [Fig. 5(F)]. Interestingly, *SOX9* expression at mRNA level was even increased with EPZ015666 [Fig. 5(E)].

PRMT5 methylates SOX9 to maintain its stability

PRMT5 seemed to regulate SOX9 at protein level rather than mRNA level. Therefore, Co-IP analysis was used to detect the interaction between PRMT5 and SOX9 and we found that PRMT5 interacted with SOX9 [Fig. 6(A) and (B)]. We also checked other molecules like RUNX2, HIF1α and FOXO3A but no interaction of PRMT5 could be detected with these molecules [Fig. 6(A)]. EPZ015666 was used to inhibit the enzyme activity of PRMT5, and *SOX9* expression was detected 24 h post treatment. As expected, *SOX9* expression was inhibited significantly [Fig. 6(C)]. These results indicate that inhibition of PRMT5 activity might accelerate SOX9 protein degradation. So, C28/I2 cells were treated with EPZ015666 to inhibit PRMT5 activity and cell lysates were immunoprecipitated with SYM10 antibody, and subsequently immunoblotted with SOX9 antibody. We found that after inhibition of PRMT5 activity, methylated SOX9 levels were significantly reduced [Fig. 6(D)]. On the other hand, the methylated SOX9 was increased with *PRMT5* overexpression [Fig. 6(E)].

We proposed that PRMT5 may stabilize SOX9 to influence the downstream gene expression. Hence, CHX was used to block protein synthesis in cells, and *SOX9* expression was detected at different time points post EPZ015666 incubation. We observed that SOX9 half-life time was significantly reduced in chondrocytes treated with PRMT5 inhibitor [Fig. 6(F)], as compared to the control group. On the other hand, SOX9 half-life time was increased in chondrocytes treated with *ad-PRMT5* as compared to the *ad-NC* group [Fig. 6(G)].

Methylated SOX9 maintains ECM homeostasis in chondrocytes

We pinpointed which arginine residue of SOX9 was methylated by PRMT5 as depicted in Table S4. Candidate positions were expected by PMeS, and a panel of single residue substitutions (R to K) were expressed as Flag-SOX9 fusion proteins. Expression of wild type (WT) *SOX9* and Flag-R74K mutant, Flag-R177K mutant, Flag-R179K mutant was observed by immunoblotting [Fig. S2(A)]. The $SOX9^{R74K}$ abrogated the transactivation of $SOX9^{wt}$, manifesting decreased *COL2A1* expression and increased *MMP-3* expression [Fig. 7(A) and (B)]. We compared the half-life time of $SOX9^{wt}$ of $SOX9^{R74K}$, $SOX9^{R177K}$, $SOX9^{R179K}$ and mixture of $SOX9^{R74K}$ and $SOX9^{wt}$. The SOX^{R74K} had a much shorter half-life compared to $SOX9^{wt}$ [Fig. 7(C) and (D)], and greater difference even occurred between $SOX9^{R74K}$ and mixture of $SOX9^{R74K}$ plus $SOX9^{wt}$. These results indicate that mutant SOX9 at the position of R74 accelerates chondrocyte ECM degradation and inhibits its stability in chondrocytes.

Discussion

Our results highlight the crucial role of PRMT5 in chondrocyte ECM metabolism. Expression of *PRMT5* is mediated by appropriate Se status, which orchestrates *SOX9* expression through methylation

the SOX9 antibody. ($n = 3$) **E.** C28/I2 cells were transfected with control adeno-virus (*ad-NC*) or *PRMT5* overexpressing adeno-virus (*ad-PRMT5*). C28/I2 cells lysates were immunoprecipitated with SYM10 and subsequently immunoblotted with SOX9 antibody. ($n = 3$) **F.** C28/I2 cells treated with or without PRMT5 inhibitor (cycloheximide, 50 μg/ml), were cultured in the complete medium for 24 h and subsequently collected at 0, 1, 2, 3, 4 and 5 h post-treatment. The lysates were immunoblotted with antibody against SOX9 (left panel). ($n = 3$) Half-life of SOX9 protein (right panel) was calculated from the data in the left panel. Intensities of IB protein bands were calculated by Image J software and normalized with GAPDH. **G.** C28/I2 cells were transfected with control adeno-virus (*ad-NC*) or PRMT5 overexpression adeno-virus (*ad-PRMT5*) for 24 h and subsequently harvested at 0, 1, 2, 3, 4 and 5 h after the treatment with cycloheximide (50 μg/ml). The lysates were immunoblotted with antibody against SOX9 (left panel). ($n = 3$) SOX9 protein half-life (right panel) was calculated from the data in the left panel**.** GAPDH was used as an internal control in immunoblotting detections. Intensities of IB protein bands were calculated by Image J software and normalized with GAPDH. Data are presented as mean ± 95 % CI of three independent experiments. All the values were obtained from the mean of three separate repeated experiment results for statistic. Data are presented as mean ± 95 % CI and analyzed using Student's *t* test for the analysis of statistical significance.

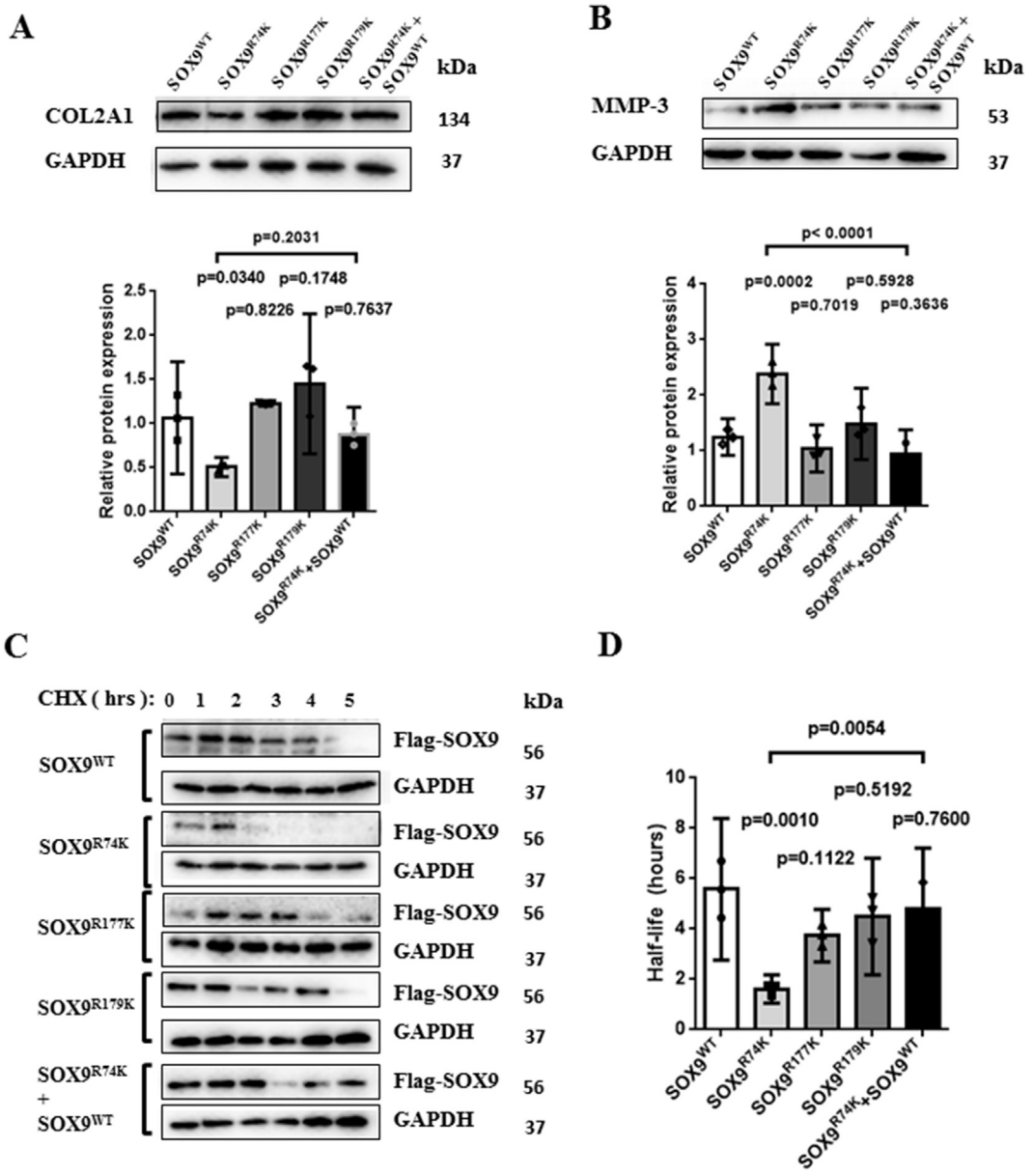

Fig. 7. PRMT5 methylates SOX9 to maintain ECM homeostasis in chondrocytes. **A.** SW1353 cells were transfected with wild type (WT) SOX9 and its mutant derivatives (1 μg). The lysates were immunoblotted with the antibodies against COL2A1. ($n = 3$) **B.** SW1353 cells were transfected with wild type (WT) SOX9 and its mutant derivatives (1 μg). The lysates were immunoblotted with the antibodies against MMP-3. ($n = 3$) **C.** SW1353 cells were transfected with wild-type (WT) SOX9 and its mutant derivatives (1 μg) for 48 hand subsequently collected at 0, 1, 2, 3, 4 and 5 h post-treatment of cycloheximide (50 μg/ml), for protein isolation. The lysates were immunoblotted with antibody against flag-SOX9. ($n = 3$) **D.** Half-life of flag-SOX9 protein was calculated from the data C. ($n = 3$) GAPDH was used as internal control in immunoblotting detections. IB protein band intensities were calculated by Image J software and normalized with GAPDH. All the values were obtained from the mean of three separate repeated experiment results for statistic. Data are presented as mean ± 95 % CI and analyzed using one-way ANOVA followed by Tukey test.

of the protein. Methylated SOX9 is essential to maintain the homeostasis of ECM. In chondrocyte exposed to Se-deficient conditions, *PRMT5* expression is inhibited, leading to lower catalysis of methyltransferase. The unmethylated SOX9 exhibits shorter half-time life resulting in increased degradation enzyme expression (Fig. 8).

In Se-deficient animal model, the typical phenotype of Se-deficiency is characterized by unbalanced cartilage ECM metabolism, epiphyseal dysplasia, delayed skeletal development, and the secondary osteoarthritis[32,37], which is consistent with KBD for its Se-deficient nutritional status[18–20]. Moreover, the main features that were observed in our Se-deficient cell model included inhibition of anabolism, that is, downregulation of COL2A1; and enhancement of catabolism, that is, upregulation of MMP-3. These findings indicate that the disorder of cartilage metabolism is a common outcome of Se-deficiency.

We inspected whether altering SBP2 can influence the degree of di-methylated proteins in chondrocytes. Surprisingly, SBP2 positively regulates the symmetric dimethyl arginine protein expression in chondrocytes [Fig. 2(A) and (B)]. Therefore, we focused on the expression of type II PRMTs in Se-deficient cells, which can form symmetric di-methyl-arginine[22,23]. Then we found that *PRMT5* expression changed significantly under different Se conditions [Fig. 3(C) and Fig. S1(D)]. It is reported that SBP2 interacts with Survival of motor neuron (SMN) complex and methylosome, which are assembled by PRMT5 for SeP mRNP assembly and translation[38]. Here, we have found a relationship among Se and PRMT5 in unbalanced chondrocytes matrix metabolism.

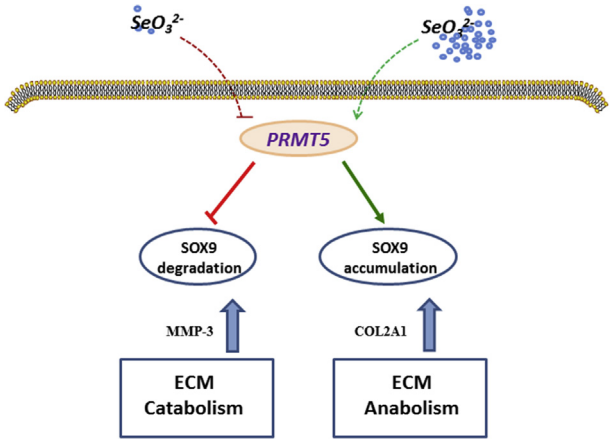

Fig. 8. A graphic molecular mechanism of Se-sensitive PRMT5 dimethylating SOX9 protein to regulate chondrocyte matrix metabolism. *PRMT5* expression is harnessed by Se status. PRMT5 functions as a catalyst to dimethylate arginine residue of SOX9. Methylated SOX9 is stabilized in the cell. Subsequently upregulated SOX9 plays crucial roles to maintain chondrocyte anabolic phenotype. If the chondrocytes are exposed to Se deficient conditions, *PRMT5* expression is inhibited, leading to degradation of SOX9. Then the balance between catabolism and anabolism is broken, which manifests the increased expression of *MMP-3* and the decreased expression of *COL2A1*.

We confirmed the role of PRMT5 by using cell experiments of gene gain or loss of function. *PRMT5* knockdown accelerated ECM degradation similar to what was observed in Se-deficiency; while *PRMT5* overexpression promoted the anabolism similar to what was observed in Se-S condition. Combined with the results from PRMT5 deficient mice[22], we believe that PRMT5 plays a key role in maintaining cartilage physiology.

The expression of matrix metabolic markers is tightly controlled by cartilage related transcriptional factors. Since PRMT5 functions as a *methyltranferase*, there is a possibility that it can modulate the expression of specific transcriptional factor(s)[39]. We found SOX9 as a substrate of PRMT5. PTM of SOX9 affects its transcriptional activity and regulates SOX9 down-stream gene expression[22,40–42]. Arginine methylation of SOX9 by PRMT4, an asymmetric dimethyltransferase enhances chondrocyte proliferation via blocking the interaction between SOX9 and beta-catenin[40]. Simultaneous mutation R74, R152, R177, R178 and R179 of SOX9 completely abolished methylation signals, whereas mutants exhibiting R177K, R178K and R179K were methylated similarly to WT, which indicates that CARM1 methylates multiple arginine residues of Sox9[13]. In our study, we could not find *PRMT4* as a Se sensitive gene, but screened the same arginine residues (R74, R177, and R179) of SOX9 could be methylated by PMeS software [Fig. S1(G) and (H)]. Mutation of R74, R177, and R179, respectively, was performed to detect *MMP-3* and *COL2A1* expression as well as the half-life time of SOX9. Results indicate that the mutation at position R74 of SOX9 accelerated *MMP-3* expression but inhibited *COL2A1* expression, which is similar to knockdown of PRMT5 or Se-deficiency condition.

In conclusion, we uncover that regulated by Se, PRMT5 stabilizes SOX9 via methylation to affect chondrocyte matrix metabolism. These findings provide a plausible explanation for Se to mediate chondrocyte matrix metabolism and unravel the novel molecular pathway of PRMT5 in cartilage.

Author contributions

Study conception and design: all authors.

Acquisition of data: Mengyao Sun, Yuxiao Hu, Yitong Zhao and Huang Huang.

Analysis and interpretation of data: Mengyao Sun, Jian Sun, and Shemin Lu.

Drafting of the manuscript: Shemin Lu, Mengyao Sun and Safdar Hussain.

Revising and final approval of the manuscript: all authors.

Conflict of interests

None declared.

Funding sources

This work was supported by grants from the National Natural Science Foundation of China (Project No. 81772410, 81671629, 81371986).

Acknowledgments

We appreciate Prof. Junling Cao for kindly providing the C28/I2 human chondrocyte line and Prof. Guihua Zhuang for giving constructive suggestions to statistic analysis. They both are from School of Public Health, Xi'an Jiaotong University Health Science Center.

Supplementary data

Supplementary data to this article can be found online at https://doi.org/10.1016/j.joca.2019.02.797.

References

1. Rayman MP. The importance of selenium to human health. Lancet 2000;356:233–41.
2. Steinbrenner H, Sies H. Protection against reactive oxygen species by selenoproteins. Biochim Biophys Acta 2009;1790:1478–85.
3. Schoenmakers E, Agostini M, Mitchell C, Schoenmakers N, Papp L, Rajanayagam O, *et al.* Mutations in the selenocysteine insertion sequence-binding protein 2 gene lead to a multisystem selenoprotein deficiency disorder in humans. J Clin Investig 2010;120:4220–35.
4. Kohrle J, Jakob F, Contempre B, Dumont JE. Selenium, the thyroid, and the endocrine system. Endocr Rev 2005;26:944–84.
5. Zamamiri-Davis F, Lu Y, Thompson JT, Prabhu KS, Reddy PV, Sordillo LM, *et al.* Nuclear factor-kappaB mediates overexpression of cyclooxygenase-2 during activation of RAW 264.7 macrophages in selenium deficiency. Free Radic Biol Med 2002;32:890–7.
6. Rayman MP. Selenium and human health. Lancet 2012;379:1256–68.
7. Allmang C, Wurth L, Krol A. The selenium to selenoprotein pathway in eukaryotes: more molecular partners than anticipated. Biochim Biophys Acta 2009;1790:1415–23.
8. Boulon S, Marmier-Gourrier N, Pradet-Balade B, Wurth L, Verheggen C, Jady BE, *et al.* The Hsp90 chaperone controls the biogenesis of L7Ae RNPs through conserved machinery. J Cell Biol 2008;180:579–95.
9. Wurth L, Gribling-Burrer AS, Verheggen C, Leichter M, Takeuchi A, Baudrey S, *et al.* Hypermethylated-capped selenoprotein mRNAs in mammals. Nucleic Acids Res 2014;42:8663–77.
10. Papp LV, Lu J, Holmgren A, Khanna KK. From selenium to selenoproteins: synthesis, identity, and their role in human health. Antioxidants Redox Signal 2007;9:775–806.
11. Kinzy SA, Caban K, Copeland PR. Characterization of the SECIS binding protein 2 complex required for the co-translational insertion of selenocysteine in mammals. Nucleic Acids Res 2005;33:5172–80.

12. Lescure A, Allmang C, Yamada K, Carbon P, Krol A. cDNA cloning, expression pattern and RNA binding analysis of human selenocysteine insertion sequence (SECIS) binding protein 2. Gene 2002;291:279–85.
13. Copeland PR, Fletcher JE, Carlson BA, Hatfield DL, Driscoll DM. A novel RNA binding protein, SBP2, is required for the translation of mammalian selenoprotein mRNAs. EMBO J 2000;19:306–14.
14. Downey CM, Horton CR, Carlson BA, Parsons TE, Hatfield DL, Hallgrimsson B, *et al.* Osteo-chondroprogenitor-specific deletion of the selenocysteine tRNA gene, Trsp, leads to chondronecrosis and abnormal skeletal development: a putative model for Kashin-Beck disease. PLoS Genet 2009;5:e1000616.
15. Moreno-Reyes R, Mathieu F, Boelaert M, Begaux F, Suetens C, Rivera MT, *et al.* Selenium and iodine supplementation of rural Tibetan children affected by Kashin-Beck osteoarthropathy. Am J Clin Nutr 2003;78:137–44.
16. Jirong Y, Huiyun P, Zhongzhe Y, Birong D, Weimin L, Ming Y, *et al.* Sodium selenite for treatment of Kashin-Beck disease in children: a systematic review of randomised controlled trials. Osteoarthritis Cartilage 2012;20:605–13.
17. Zou K, Liu G, Wu T, Du L. Selenium for preventing Kashin-Beck osteoarthropathy in children: a meta-analysis. Osteoarthritis Cartilage 2009;17:144–51.
18. Stone R, Diseases. A medical mystery in middle China. Science 2009;324:1378–81.
19. Cao J, Li S, Shi Z, Yue Y, Sun J, Chen J, *et al.* Articular cartilage metabolism in patients with Kashin-Beck Disease: an endemic osteoarthropathy in China. Osteoarthritis Cartilage 2008;16:680–8.
20. Duan C, Guo X, Zhang XD, Yu HJ, Yan H, Gao Y, *et al.* Comparative analysis of gene expression profiles between primary knee osteoarthritis and an osteoarthritis endemic to Northwestern China, Kashin-Beck disease. Arthritis Rheum 2010;62:771–80.
21. Speckmann B, Grune T. Epigenetic effects of selenium and their implications for health. Epigenetics 2015;10:179–90.
22. Norrie JL, Li Q, Co S, Huang BL, Ding D, Uy JC, *et al.* PRMT5 is essential for the maintenance of chondrogenic progenitor cells in the limb bud. Development 2016;143:4608–19.
23. Enomoto H, Enomoto-Iwamoto M, Iwamoto M, Nomura S, Himeno M, Kitamura Y, *et al.* Cbfa1 is a positive regulatory factor in chondrocyte maturation. J Biol Chem 2000;275:8695–702.
24. Djouad F, Bony C, Canovas F, Fromigue O, Reme T, Jorgensen C, *et al.* Transcriptomic analysis identifies Foxo3A as a novel transcription factor regulating mesenchymal stem cell chrondrogenic differentiation. Clon Stem Cells 2009;11:407–16.
25. Duval E, Leclercq S, Elissalde JM, Demoor M, Galera P, Boumediene K. Hypoxia-inducible factor 1alpha inhibits the fibroblast-like markers type I and type III collagen during hypoxia-induced chondrocyte redifferentiation: hypoxia not only induces type II collagen and aggrecan, but it also inhibits type I and type III collagen in the hypoxia-inducible factor 1alpha-dependent redifferentiation of chondrocytes. Arthritis Rheum 2009;60:3038–48.
26. Zheng Q, Zhou G, Morello R, Chen Y, Garcia-Rojas X, Lee B. Type X collagen gene regulation by Runx2 contributes directly to its hypertrophic chondrocyte-specific expression in vivo. J Cell Biol 2003;162:833–42.
27. Bell DM, Leung KK, Wheatley SC, Ng LJ, Zhou S, Ling KW, *et al.* SOX9 directly regulates the type-II collagen gene. Nat Genet 1997;16:174–8.
28. Majumdar MK, Askew R, Schelling S, Stedman N, Blanchet T, Hopkins B, *et al.* Double-knockout of ADAMTS-4 and ADAMTS-5 in mice results in physiologically normal animals and prevents the progression of osteoarthritis. Arthritis Rheum 2007;56:3670–4.
29. Neuhold LA, Killar L, Zhao W, Sung ML, Warner L, Kulik J, *et al.* Postnatal expression in hyaline cartilage of constitutively active human collagenase-3 (MMP-13) induces osteoarthritis in mice. J Clin Investig 2001;107:35–44.
30. Hwang HS, Park SJ, Cheon EJ, Lee MH, Kim HA. Fibronectin fragment-induced expression of matrix metalloproteinases is mediated by MyD88-dependent TLR-2 signaling pathway in human chondrocytes. Arthritis Res Ther 2015;17:320.
31. Homandberg GA, Hui F. Association of proteoglycan degradation with catabolic cytokine and stromelysin release from cartilage cultured with fibronectin fragments. Arch Biochem Biophys 1996;334:325–31.
32. Min Z, Zhao W, Zhong N, Guo Y, Sun M, Wang Q, *et al.* Abnormality of epiphyseal plate induced by selenium deficiency diet in two generation DA rats. APMIS 2015;123:697–705.
33. Min Z, Guo Y, Sun M, Hussain S, Zhao Y, Guo D, *et al.* Selenium-sensitive miRNA-181a-5p targeting SBP2 regulates selenoproteins expression in cartilage. J Cell Mol Med 2018;22(12):5888–98.
34. Yan J, Tian J, Zheng Y, Han Y, Lu S. Selenium promotes proliferation of chondrogenic cell ATDC5 by increment of intracellular ATP content under serum deprivation. Cell Biochem Funct 2012;30:657–63.
35. Yan J, Zheng Y, Min Z, Ning Q, Lu S. Selenium effect on selenoprotein transcriptome in chondrocytes. Biometals 2013;26:285–96.
36. Boisvert FM, Cote J, Boulanger MC, Cleroux P, Bachand F, Autexier C, *et al.* Symmetrical dimethylarginine methylation is required for the localization of SMN in Cajal bodies and pre-mRNA splicing. J Cell Biol 2002;159:957–69.
37. Ren FL, Guo X, Zhang RJ, Wang Sh J, Zuo H, Zhang ZT, *et al.* Effects of selenium and iodine deficiency on bone, cartilage growth plate and chondrocyte differentiation in two generations of rats. Osteoarthritis Cartilage 2007;15:1171–7.
38. Gribling-Burrer AS, Leichter M, Wurth L, Huttin A, Schlotter F, Troffer-Charlier N, *et al.* SECIS-binding protein 2 interacts with the SMN complex and the methylosome for selenoprotein mRNP assembly and translation. Nucleic Acids Res 2017;45:5399–413.
39. Cho EC, Zheng S, Munro S, Liu G, Carr SM, Moehlenbrink J, *et al.* Arginine methylation controls growth regulation by E2F-1. EMBO J 2012;31:1785–97.
40. Ito T, Yadav N, Lee J, Furumatsu T, Yamashita S, Yoshida K, *et al.* Arginine methyltransferase CARM1/PRMT4 regulates endochondral ossification. BMC Dev Biol 2009;9:47.
41. Hattori T, Eberspaecher H, Lu J, Zhang R, Nishida T, Kahyo T, *et al.* Interactions between PIAS proteins and SOX9 result in an increase in the cellular concentrations of SOX9. J Biol Chem 2006;281:14417–28.
42. Akiyama H, Kamitani T, Yang X, Kandyil R, Bridgewater LC, Fellous M, *et al.* The transcription factor Sox9 is degraded by the ubiquitin-proteasome system and stabilized by a mutation in a ubiquitin-target site. Matrix Biol 2005;23:499–505.